

Article

Comparison of Four Immobilization Methods for Different Transaminases

Tobias Heinks ¹, Nicolai Montua ^{2,†}, Michelle Teune ^{1,3,†}, Jan Liedtke ¹, Matthias Höhne ⁴,
Uwe T. Bornscheuer ³ and Gabriele Fischer von Mollard ^{1,*}

¹ Faculty of Chemistry, Biochemistry, Bielefeld University, Universitätsstr. 25, 33615 Bielefeld, Germany

² Faculty of Chemistry, Organic and Bioorganic Chemistry, Bielefeld University, Universitätsstraße 25, 33615 Bielefeld, Germany

³ Department of Biotechnology and Enzyme Catalysis, Institute of Biochemistry, University of Greifswald, Felix Hausdorff-Str. 4, 17487 Greifswald, Germany

⁴ Protein Biochemistry, Institute of Biochemistry, University of Greifswald, Felix Hausdorff-Str. 4, 17487 Greifswald, Germany

* Correspondence: gabriele.mollard@uni-bielefeld.de

† These authors contributed equally to this work.

Abstract: Biocatalytic syntheses often require unfavorable conditions, which can adversely affect enzyme stability. Consequently, improving the stability of biocatalysts is needed, and this is often achieved by immobilization. In this study, we aimed to compare the stability of soluble and immobilized transaminases from different species. A cysteine in a consensus sequence was converted to a single aldehyde by the formylglycine-generating enzyme for directed single-point attachment to amine beads. This immobilization was compared to cross-linked enzyme aggregates (CLEAs) and multipoint attachments to glutaraldehyde-functionalized amine- and epoxy-beads. Subsequently, the reactivity and stability (i.e., thermal, storage, and solvent stability) of all soluble and immobilized transaminases were analyzed and compared under different conditions. The effect of immobilization was highly dependent on the type of enzyme, the immobilization strategy, and the application itself, with no superior immobilization technique identified. Immobilization of HA_{GA}-beads often resulted in the highest activities of up to 62 U/g beads, and amine beads were best for the hexameric transaminase from *Luminiphilus sylvensis*. Furthermore, the immobilization of transaminases enabled its reusability for at least 10 cycles, while maintaining full or high activity. Upscaled kinetic resolutions (partially performed in a SpinChem™ reactor) resulted in a high conversion, maintained enantioselectivity, and high product yields, demonstrating their applicability.

Keywords: amine transaminase; enzyme stability; enzyme immobilization; site-selective immobilization; reusability; storage stability; thermostability; operational stability; solvent stability; formylglycine-generating enzyme



check for updates

Citation: Heinks, T.; Montua, N.; Teune, M.; Liedtke, J.; Höhne, M.; Bornscheuer, U.T.; Fischer von Mollard, G. Comparison of Four Immobilization Methods for Different Transaminases. *Catalysts* **2023**, *13*, 300. <https://doi.org/10.3390/catal13020300>

Academic Editors: Yihan Liu and Liang Zhang

Received: 15 December 2022

Revised: 16 January 2023

Accepted: 24 January 2023

Published: 28 January 2023



Copyright: © 2023 by the authors. Licensee MDPI, Basel, Switzerland. This article is an open access article distributed under the terms and conditions of the Creative Commons Attribution (CC BY) license (<https://creativecommons.org/licenses/by/4.0/>).

1. Introduction

Amine transaminases (ATAs) catalyze the amine transfer from an amine donor to an acceptor substrate via its cofactor pyridoxal-5'-phosphate (PLP). These enzymes are highly enantioselective and are therefore widely used to produce enantiomerically pure chiral amines in single or cascade reactions, which are precursors for a variety of drugs, such as (*R*)-sitagliptin (antidiabetic drug) [1], (*S*)-rivastigmine (Alzheimer's and Parkinson's disease treatment) [2], or (*R*)-ramatroban (antiallergic drug) [3]. In 2014, 40% of pharmaceuticals were estimated to contain an amine functionality [4], showing the importance of chiral amines as a functional group. Therefore, the production of these precursors and subsequently of these pharmaceuticals using biocatalysts such as transaminases, is of great interest. However, there are still obstacles to using transaminases in industrial applications and transferring laboratory experiments to industrial-scale productions can

be challenging. Limitations arise from product inhibition and instabilities under harsh reaction conditions, such as high reaction temperatures, extreme pH, high shear forces, high substrate and product concentrations, various solvents, undesirable reaction equilibria, and low operational stability [5–10]. In addition, product separation becomes more difficult with an increasing volume, and the soluble biocatalysts usually become unusable after product extraction, resulting in high costs for enzyme production. To tackle these problems, protein immobilization has received increasing attention over the recent decades, because immobilized biocatalysts provide several advantages, such as easier removal from product solutions, re-use in multiple batch reactions, modification of their properties (e.g., extending the pH range for optimal reactions), and higher (operational) stability and activity [6,11–19]. However, each biocatalyst behaves differently upon immobilization, and there are also enzymes that have been destabilized [20–23]. Thus, immobilization must be established experimentally for each protein, and the optimal conditions are rarely transferable to other proteins. Moreover, different immobilization strategies are possible, with each technique having its own advantages or disadvantages.

A general distinction regarding protein immobilization is made between a covalent binding to solid supports, physical adsorption (e.g., via hydrophobic or ionic interactions), enzyme entrapment (mainly in gel matrices), and the cross-linking of enzymes with each other to obtain cross-linked enzyme aggregates (CLEAs). Several protocols for immobilization via CLEAs [24–27] and on solid supports via multiple binding [28–33] have been reported. Covalent immobilization by a multi-point attachment was realized, for example, by using supports that expose epoxy groups [28,34,35] or functionalized amine groups with glutaraldehyde [36–39], bisepoxides [28,35], or other difunctional reagents [40]. Site-specific immobilization enables targeted immobilization and can avoid detrimental binding (e.g., if the catalytic site is facing the surface), excessive enzyme rigidification, and unspecific interactions (e.g., with active site amino acids). This immobilization is often achieved by addressing, for example, the His-tag [41,42], or by various other techniques [43–47]. In this study, the rarely used aldehyde-tag system was used, which exposes a cysteine residue within its consensus sequence to a formylglycine-generating enzyme (FGE) [48,49]. Upon the conversion of the cysteine to a unique C-formylglycine, the exposed aldehyde functionality can be addressed by common amine-exposing beads. Consequently, only a small tag is incorporated into the protein sequence, which has less impact on enzymatic structures and allows stable bonds instead of non-covalent interactions, as in the case of His-tags. Furthermore, this technique is based on biocatalytic rather than chemical modification, and the FGE applied is potentially reusable [50].

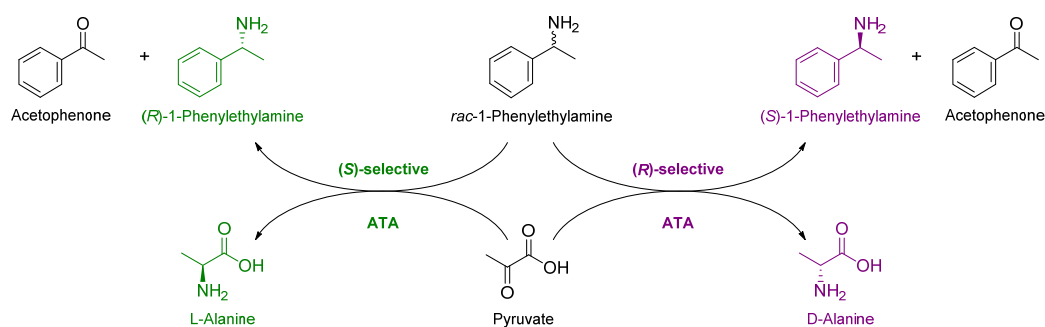
To date, several ATAs have been immobilized that can yield recyclable and robust biocatalysts [11,33,51–53]. For example, ATAs have been successfully immobilized covalently on various supports [33,35,46,53], by ionic or hydrophobic interactions [16,52] and by encapsulation in whole cells [54,55]. Although enzyme immobilization is often associated with improvements of enzyme properties, the catalytic properties and stabilities of transaminases are often not drastically altered [33,53,56–59]. Therefore, the aim of this study was to comprehensively characterize four different ATAs in terms of their reaction behavior and stability, before and after immobilization. ATA-Vfl is a dimeric, (S)-selective wildtype transaminase from *Vibrio fluvialis*, and it has been frequently examined and used in several studies [60–64]. ATA-Bmu is an (S)-selective wildtype transaminase from *Burkholderia multivorans*, and was recently discovered by database mining as a member of the β -alanine:pyruvate transaminase family [65]. Enzymes of this family exhibit a tetrameric structure associated with high operational stability. ATA-3FCR-5M is a dimeric, (S)-selective mutant of the transaminase from *Ruegeria* sp. TM1040 (PDB-code: 3FCR), which has been the target of numerous protein engineering approaches following the discovery of its structure and characterization studies in 2012 [66,67]. It has been engineered to accept a wider range of bulky substrates with high selectivity and activity [68]. However, due to stability issues based on one amino acid substitution, the most active transaminase (ATA-3FCR-5M) was discarded, and the second most active transaminase, carrying only

four substitutions (ATA-3FCR-4M), was used for synthesis. ATA-Lsy is a wildtype transaminase from *Luminiphilus sylvensis* NOR5-1B, and was discovered in 2010 as an (*R*)-selective transaminase [69]. In 2021 ATA-Lsy was determined to be a hexameric protein composed of three dimers, and it was further engineered to accept larger substrates [70]. Little to no in-depth information has been published on the stability of soluble and immobilized ATA-Bmu, ATA-3FCR-5M, and ATA-Lsy. Hence, these four selected transaminases allow us to analyze the differences between enzymes with different enantiopreferences and with different numbers of subunits (dimer vs. tetramer vs. hexamer). Furthermore, the effect of four different immobilization strategies on the transaminases can be analyzed.

2. Results and Discussion

2.1. Immobilization of the Transaminases

All ATAs were immobilized using four different strategies: immobilization (i) on epoxy (EP)-beads, (ii) on amine (HA)-beads, (iii) on glutaraldehyde functionalized amine (HA_{GA})-beads, and (iv) via cross-linking of enzyme aggregates (CLEAs). This allowed differences to be analyzed between multi-point (methods i, iii, and iv) and site-selective oriented single-point attached proteins (method ii), as well as between support-dependent (methods i-iii) and -independent (method iv) applications. Transaminases with aldehyde-tags were only used in the case of HA-bead immobilization. An extensive screening of the different immobilization conditions was first performed to determine the optimal conditions for each protein and strategy (Figure S1). The activity of soluble and immobilized transaminases was always (unless otherwise stated) determined using the acetophenone assay [71], in which the formation of acetophenone was followed within the kinetic resolution of racemic 1-phenylethylamine (*rac*-1-PEA (Scheme 1)).



Scheme 1. Kinetic resolution of racemic 1-phenylethylamine. To determine the activity of soluble and immobilized transaminases, the acetophenone assay [71] was used in this study, in which the kinetic resolution of racemic 1-phenylethylamine (*rac*-1-PEA) is followed by the photometric detection of the product, acetophenone, at 245 nm. Pyruvate is used as co-substrate. Using (*S*)-selective transaminases, (*R*)-1-PEA as well as L-alanine are obtained as products (green), whereas using (*R*)-selective transaminases leads to (*S*)-1-PEA and D-alanine (purple).

First, the effect of the pH (pH 5.0, 7.5, 9.0, and 10.5) was investigated. Both extremely high and low pH values are frequently associated with protein denaturation [72–74]. For example, we have recently demonstrated that a pH of 5.0 has a strong denaturing and inactivating effect on ATA-Vfl in a solution [46]. However, immobilization via aldehyde coupling (HA and HA_{GA}) was often favored at an acidic pH (Table S1), suggesting that immobilization prevents the denaturation and aggregation of the transaminases. In contrast, this type of immobilization (i.e., via lysine residues) is generally recommended using a neutral or basic pH [46,75,76]. The coupling to epoxy beads was less pH-dependent (pH 5.0–7.5 and 10.5). Next, the duration of immobilization (4, 8, 16, and 24 h) was studied. It became clear that aldehyde/formylglycine coupling appeared to be a rapid immobilization technique, as all transaminases (except ATA-Vfl) showed the highest activities after 4 h of immobilization, whereas longer periods led to stagnating or decreasing activities.

In contrast, epoxy immobilization required longer immobilization times. The latter can be explained by the highly hydrophobic nature of the epoxy-beads, requiring additional additives to reduce the repulsion between beads and proteins, and to bring them into spatial proximity in the first step, and allow immobilization in the second step. These additives should be gentle to the proteins. High amounts of sodium phosphate (0.5 M) or ammonium sulfate (50–75%) were sufficient for these transaminases. The immobilization temperature (4, 22, and 37 °C) was also analyzed, as it may accelerate immobilization on the one hand, but also may destabilize the proteins. The ideal temperature appeared to be protein-dependent. Epoxy immobilization generally required higher temperatures, possibly due to higher kinetic energies accelerating the slow immobilization reaction. Finally, the optimal amount of protein applied per mg of beads was also dependent on the protein and technique.

In the case of CLEA-formation, a neutral pH of 7.5 and a standard immobilization time (1 h precipitation, 4 h cross-linking) was chosen, as these conditions have been recommended in various protocols [24,25], which we also confirmed in initial tests (data not shown). In a first attempt, an extensive screening of precipitants was required, as the protein should be recoverable in an active soluble form upon resolubilization, indicating a similar active conformation in the precipitates. The type of precipitant was dependent on the transaminase used, as it showed different effects on the activity of the solubilized enzymes. Nevertheless, conditions could be established for all the transaminases (Table S1). Subsequently, two different cross-linkers (glutaraldehyde (GA) and divinyl sulfone (DVS)) were analyzed in combination with the best precipitants. In general, low concentrations of the cross-linkers were optimal, while higher concentrations decreased the activity in most cases, with glutaraldehyde being the cross-linker of choice for three enzymes. The inactivation at higher concentrations could be due to (i) the binding to the catalytic lysine within the active site, (ii) the modification of the cofactor, (iii) a high degree of crowding whereby inner enzymes become inaccessible to substrates, or (iv) an excessive degree of intra- and intermolecular coupling, limiting the enzyme's flexibility, which could negatively affect catalytic activity.

Having established the optimal immobilization conditions (Table S1), immobilization with 40 mg beads was performed to determine various immobilization parameters that can be used to evaluate the quality of enzyme immobilization (Table S2). The total activity of all immobilizates was determined under standard conditions (50 mM Tris buffer, 0.1 mM PLP, pH 8.0) and the best immobilizate was defined based on the total specific activity of the immobilizates (Table 1, highlighted in bold).

Table 1. Specific activity, binding efficiency, and activity recovery of immobilized transaminase on solid supports. The best immobilizates of the transaminases on solid support are defined as immobilizates with the highest activity (U/g bead) and are highlighted in bold. Activity recovery was determined as indicated in the Supplementary Materials, where also the complete and detailed immobilization parameters can be found (Table S2).

Transaminase	Type	Specific Activity of Biocatalyst [U/g bead] ¹	Binding Efficiency [%] ²	Activity Recovery [%] ³
ATA-Vfl	HA	53	97.6	6
	HA_{GA}	62	52.7	7
	EP	49	64.0	5
ATA-Bmu	HA	26	97.1	17
	HA_{GA}	55	69.3	19
	EP	26	97.7	20
ATA-3FCR-5M	HA	44	95.4	15
	HA_{GA}	44	98.2	50
	EP	15	77.3	2

Table 1. Cont.

Transaminase	Type	Specific Activity of Biocatalyst [U/g bead] ¹	Binding Efficiency [%] ²	Activity Recovery [%] ³
ATA-Lsy	HA	48	46.9	15
	HA _{GA}	34	94.6	16
	EP	36	62.6	12

¹ The specific activity of biocatalyst is the observed activity of the immobilized enzyme per g of bead support (specific activity of the immobilizates). ² Binding efficiency is the percentage ratio between the total amount of immobilized enzyme (protein amount in the starting solution minus protein amount in the supernatant) and the total protein amount initially applied with the starting solution. ³ Activity recovery is the percentage ratio between the observed activity of the immobilizate (in units) and the activity initially applied for the immobilization (in units).

The activity recoveries of the transaminases ATA-Bmu, ATA-3FCR-5M, and ATA-Lsy were comparable to other transaminase immobilizations that yielded activity recoveries in a wide range between 0.5 and 87% [17,33,34,53,77,78]. In the case of ATA-Vfl, lower activity recoveries were observed. However, in only two out of six immobilization studies known to us [32,46,53,59,79,80], the activity recovery of ATA-Vfl was determined and varied between 0.5 and 17.8% in one study [53], and 3 and 37% in another study [59]. The wide range of activity recoveries in all cited publications and in our results demonstrate the dependence on the immobilization supports, the enzymes, and further optimization (e.g., addition of glycerol [59]). However, the activity recovery was mostly below 50%, which might be due to the oligomeric state of the transaminases and the association with PLP.

2.2. Effect of Immobilization: Reactivities and Stabilities of Soluble and Immobilized Transaminases

Next, different stabilities and reactivities under several conditions for the four transaminases in soluble and immobilized forms were analyzed (for detailed information, see Supplementary Materials and methods). Since immobilization had the greatest effect on ATA-Bmu, we selected this transaminase to highlight and compare the reactivities and stabilities of the soluble and immobilized forms in detail. All other data regarding ATA-Vfl, ATA-Lsy, and ATA-3FCR-5M are shown in detail in the Supplementary Materials.

The (S)-selective ATA from *Burkholderia multivorans* (ATA-Bmu) was classified in a recent publication to be an operationally stable transaminase that can withstand operating temperatures of 60 °C for 20 h in the presence of 25–50%(v/v) co-solvents at 30 °C [65]. However, ATA-Bmu proved to be unstable when stored for a long time at 4 °C (Figure 1a): The enzyme showed a significant loss of activity during storage for 56 days (5% residual activity) under standard storage conditions (pH 8.0, bicine buffer, 0.1 mM PLP, 4 °C, dark, and exposed to air). The use of different pH, buffers, and temperatures did not increase the storage stability, whereas the addition of >25% ammonium sulfate (31%) or 10 mM pyruvate (27%) increased it to a small extent (Figure 1b,c). Notably, ATA-Bmu was strongly stabilized by immobilization: The immobilized enzyme retained up to 66% activity after 56 days of storage under standard conditions, whereas the type of immobilization played only a minor role (45–66% residual activity, Figure 1a). Moreover, immobilization even allowed ATA-Bmu to be stored at 20 °C, in different buffers and at different pH (Figure 1b), and under operating conditions (addition of 1-PEA and alanine, Figure 1c) with increased stability. A single-event immobilization on the HA-beads via the FGly-Tag provided the highest storage stability, and 87% and 107% residual activity could be achieved if stored under standard storage conditions (pH 8.0, 0.1 mM PLP, 4 °C, dark, exposed to air) in the HEPES buffer, without additives and with 50% (NH₄)₂SO₄, respectively (Figure 1b,c). Ketones had no drastic effect on the stability of immobilized ATA-Bmu. In contrast, the storage in the Tris buffer (other buffers showed no significant effects) and at a pH of 10 was detrimental to all transaminases (Figure 1b and Figure S2b-panels), suggesting that the Tris buffer, with its primary amine functionality and a basic pH, should be avoided for the long-term storage of transaminases.

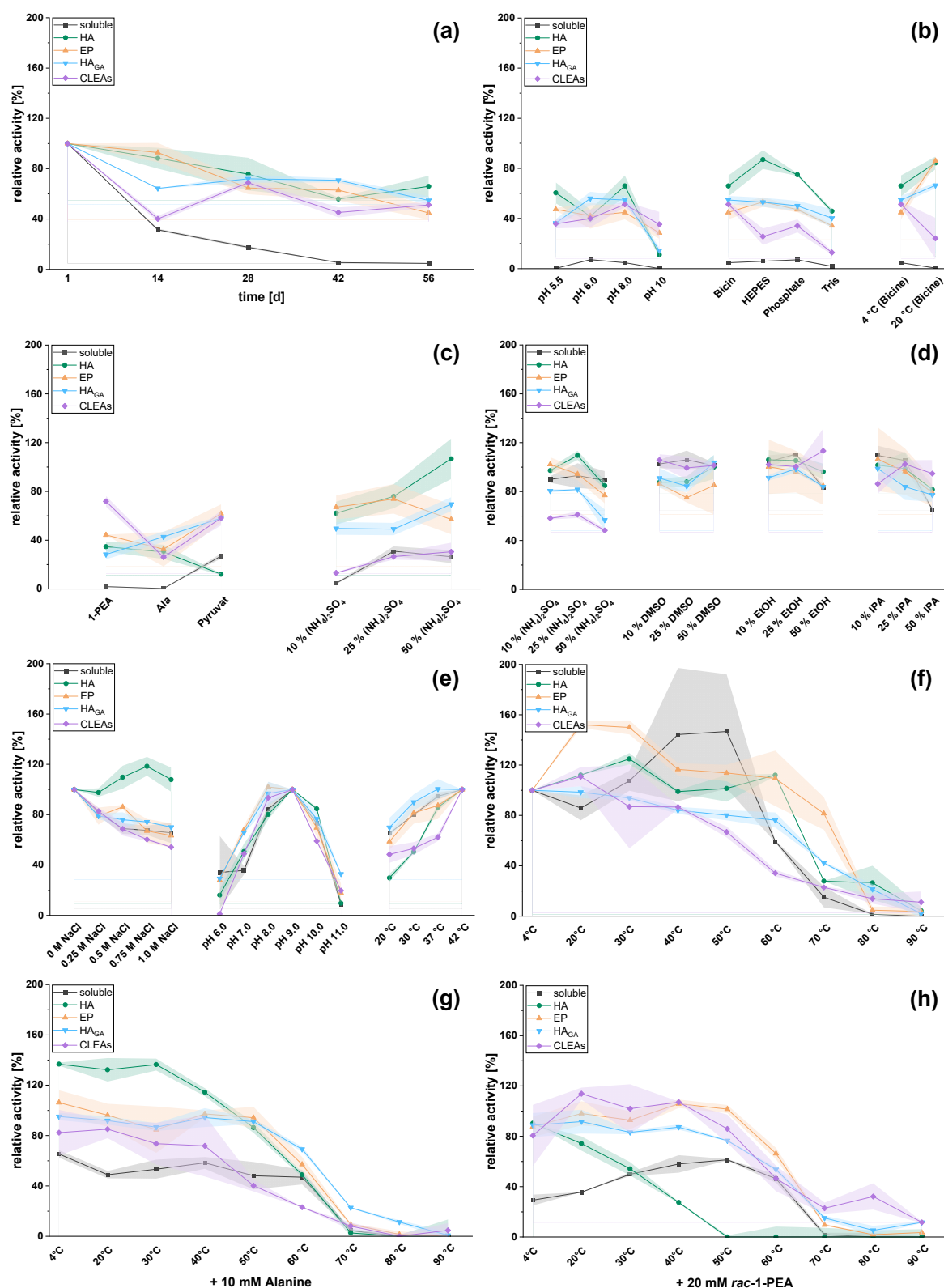


Figure 1. Stability and reactivity of ATA-Bmu under different conditions. Stabilities and activities of soluble ATA-Bmu (black) and immobilized ATA-Bmu (on HA-beads (green), EP-beads (yellow), HA_{GA}-beads (blue) or as CLEAs (purple)) were analyzed under different conditions: (a) storage stability under standard storage conditions (pH 8.0, bicine buffer, 0.1 mM PLP, 4°C, dark, and exposed to air), (b,c) storage stability over 56 days under various conditions (different pH, buffer, and additives) while the standard storage conditions (see before) were fixed except for the varied

condition, (d) resting solvent stability after storage at room temperature for 6 h with different additives, (e) reactivity at different salt concentrations, pH, and temperatures, while the standard reaction conditions (see below) were fixed except for the varied condition, and (f–h) thermostability: incubation for 6 h without additives and with alanine or racemic 1-phenylethylamine (*rac*-1-PEA) at different temperatures. In all cases except (e), the immobilizates were washed thoroughly (3 times with 50 mM Tris, 0.1 mM PLP) and the activity was subsequently detected under standard reaction conditions (50 mM Tris pH 8.0, 0.5% DMSO, 0.1 mM PLP, 2.5 mM *rac*-1-PEA, and 2.5 mM pyruvate). All reactions were conducted in duplicates and the standard deviations are shown as filled areas. Further information can be obtained from the Supplementary Materials (Section S2) and methods.

ATA-Bmu was thermostable in a soluble and immobilized form, showing a remaining activity up to 60 °C (Figure 1f). Furthermore, ATA-Bmu was the most thermostable transaminase in this study under operating conditions: the transaminase retained high activities up to 60 °C, which was at least 20 °C higher than the other transaminases, regardless of whether alanine or 1-PEA was used (Figure 1g,h). In general, the high thermostability was maintained by all immobilization techniques under resting conditions (Figure 1f). Interestingly, the activities were significantly higher under operational conditions in the presence of alanine and 1-PEA after immobilization (Figure 1g,h, respectively). Hence, the immobilizates can be used at high reaction temperatures with high activities.

Overall, the optimal reaction conditions for ATA-Bmu have been a neutral to basic pH (9.0), low ionic strength (0 M NaCl), and an elevated reaction temperature (42 °C) (Figure 1e). This could be observed for several transaminases in the literature [81–83] and all transaminases in this study (Figure S2e-panels). Interestingly, immobilization on HA-beads resulted in a higher salt-tolerance. In addition, the storage of the transaminase immobilizates in dried form was not successful, as the activity decreased by 75–85% (Figure S4).

The activity of enzymes in the presence of different solvents is a crucial issue for (industrial) synthesis. For example, in one study, a substrate had to be solubilized in 20% isopropanol with the enzyme still active [84]. ATA-Bmu was shown to withstand different solvents, such as the use of isopropanol or acetonitrile, and maintain a high activity as a soluble protein [65]. This was also observed in this study, using different solvents under resting (residual activity after 6 h incubation with solvents at room temperature, Figure 1d) and operating conditions (activity in the presence of different solvents, Figure 2a). In the case of the resting solvent stabilities, no significant differences were observed after immobilization. In contrast, immobilization of ATA-Bmu resulted in slightly lower operating stabilities in DMSO and isopropanol, while no significant change was obtained in ethanol and a slight increase was found in acetonitrile (ACN). These minor effects of immobilization might be due to the already high solvent stability of soluble ATA-Bmu.

In contrast, immobilization positively affected the operational stabilities of ATA-Vfl, ATA-3FCR-5M, and ATA-Lsy in the presence of organic solvents (Figure 2b–d). Soluble ATA-Vfl showed a limited tolerance toward DMSO and ACN and higher concentrations ($\geq 25\%$) of ethanol and isopropanol. Immobilization stabilized the enzyme in the presence of almost all solvents. Compared to soluble ATA-Vfl, the activities of most immobilizates were greatly increased in the presence of 10% ethanol, 10% isopropanol, and up to 50% DMSO. Immobilization on HA-beads resulted in the highest activities in DMSO and ethanol at all concentrations, and 25% ACN. ATA-3FCR-5M showed surprisingly high stabilities as a soluble enzyme but was inactive in 25 and 50% ethanol. In most cases, the immobilization of ATA-3FCR-5M did increase or maintain the stability toward these solvents. The high stability in DMSO was maintained only by CLEA-immobilization, which gave the highest activities in most cases. All immobilizates had strongly increased activities in ethanol compared to the soluble enzyme. ATA-Lsy showed high resting solvent stability (higher than ATA-Bmu in some cases Figure S2), which might be explained by its hexameric structure. However, the operational solvent stabilities were the lowest in the case of ethanol (no activity at all concentrations) and isopropanol (no activity at

concentrations above 10%), indicating a high sensitivity to alcohols. The immobilization of ATA-Lsy generally resulted in higher activities, especially in the alcohols, so that the reaction could be performed with ethanol or isopropanol up to a concentration of 50%. The activity in 50% DMSO was strongly increased by immobilization on HA-beads. In the case of ACN, the activity was further increased by immobilization on HA- and EP-beads. The immobilization on HA-beads stabilized ATA-Lsy the most, while CLEA-immobilizates resulted in the lowest activities.

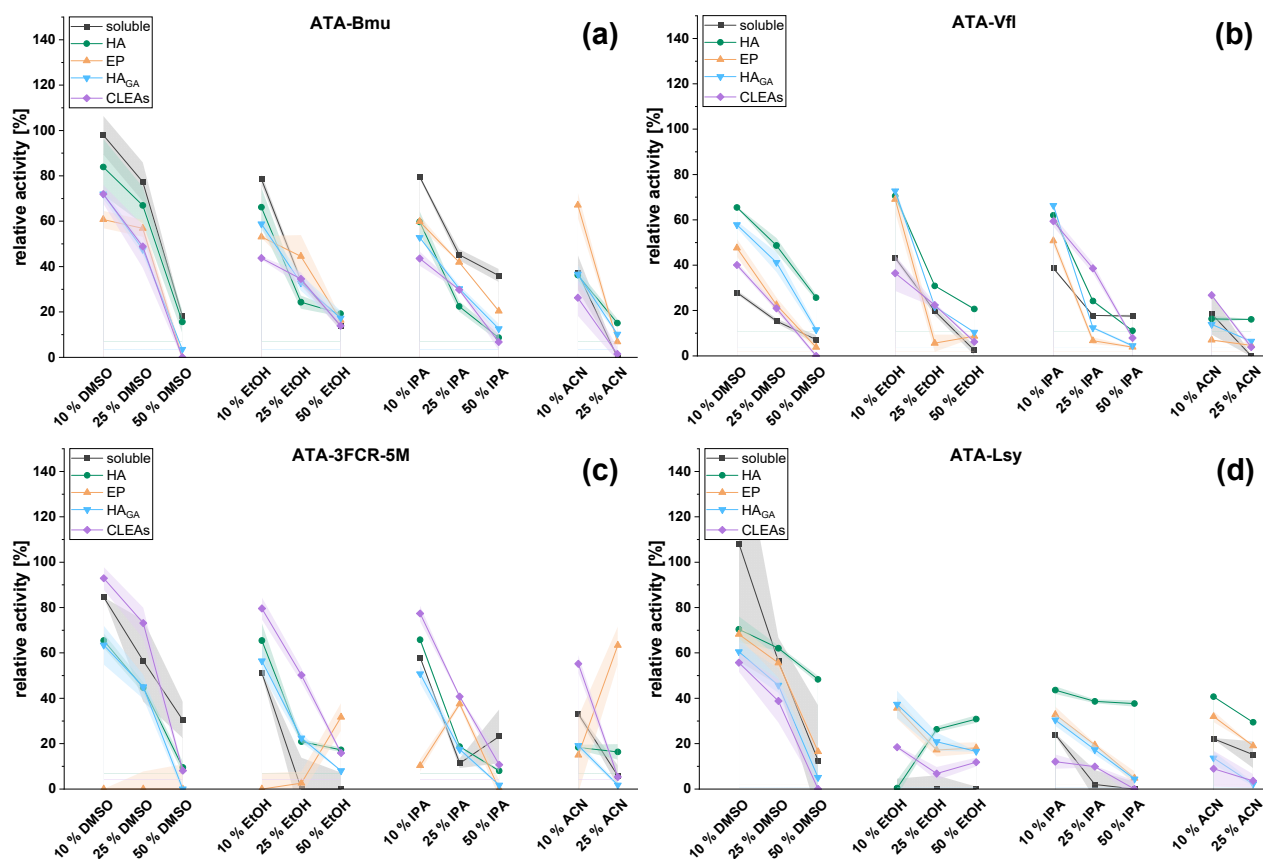


Figure 2. Operational solvent stabilities of different transaminases. Several solvents (DMSO, ethanol (EtOH), isopropanol (IPA), and acetonitrile (ACN)) were added in different concentrations (10, 25, and 50%) to the standard reaction solution (see below) of all transaminases and immobilizates: (a) ATA-Bmu, (b) ATA-Vfl, (c) ATA-3FCR-5M, and (d) ATA-Lsy. The activity without additives (standard reaction solution for all ATAs: 50 mM Tris pH 8.0, 0.5% DMSO, 0.1 mM PLP, 2.5 mM *rac*-1-PEA, and 2.5 mM pyruvate) was set as 100%, and the standard deviation of duplicates is shown as filled area.

2.3. Reusability of Immobilized Transaminases

An important advantage of immobilized proteins is their reusability in multiple cycles of product synthesis. Therefore, the reusability of all transaminase-immobilizates was analyzed in kinetic resolutions of *rac*-1-PEA (Figure 3) as a model reaction. The reactions were performed at 37 °C for 45 min, after which the reaction solution (50 mM Tris, 0.1 mM PLP, 0.5% DMSO, 2.5 mM *rac*-1-PEA, 2.5 mM pyruvate, and pH 8.0) was separated and analyzed. The immobilizates were then washed (2 times with 50 mM Tris, 0.1 mM PLP) and reused in a new batch reaction.

ATA-Bmu retained its full activity when immobilized on EP- or HA_{GA}-beads, whereas the activity decreased when it was immobilized on HA-beads (65% residual activity) or CLEAs (28% residual activity, Figure 3a). ATA-Vfl was very stable, independent of the immobilization method for a minimum of 10 recycling steps, retaining nearly full activity (Figure 3b). ATA-Lsy maintained its full activity for all immobilizates in all cycles, except

for ATA-Lsy-CLEAs with a residual activity of 53% (Figure 3d). On the other hand, all immobilizates of ATA-3FCR-5M were not so stable, resulting in residual activities of 48% (HA_{GA}-beads), 30% (EP-beads) 22% (HA-beads), and 45% (CLEAs, Figure 3c). Interestingly, the recycling stability for ATA-Bmu was higher when immobilized via multipoint attachment strategies on solid supports (EP and HA_{GA}) than when immobilized via a single bond per subunit (HA) or as CLEAs. The immobilization of enzymes via multipoint attachments is generally found to be more stable to external influences [75,85,86], which might improve the reusability of some enzymes. In addition, for transaminases, the dissociation of dimers upon the loss of the cofactor leaving inactive enzymes [7,87,88] might be reduced, leading to higher operational stability and thus, better reusability. On the other hand, if the enzymes are too densely packed, rigidified, and overcrowded, which is likely to occur in CLEAs and on beads, the total activity might decrease [85]. This was also observed when the transaminases immobilized on beads were post-cross-linked (Figure S3), which was initially analyzed to prevent dimer dissociation.

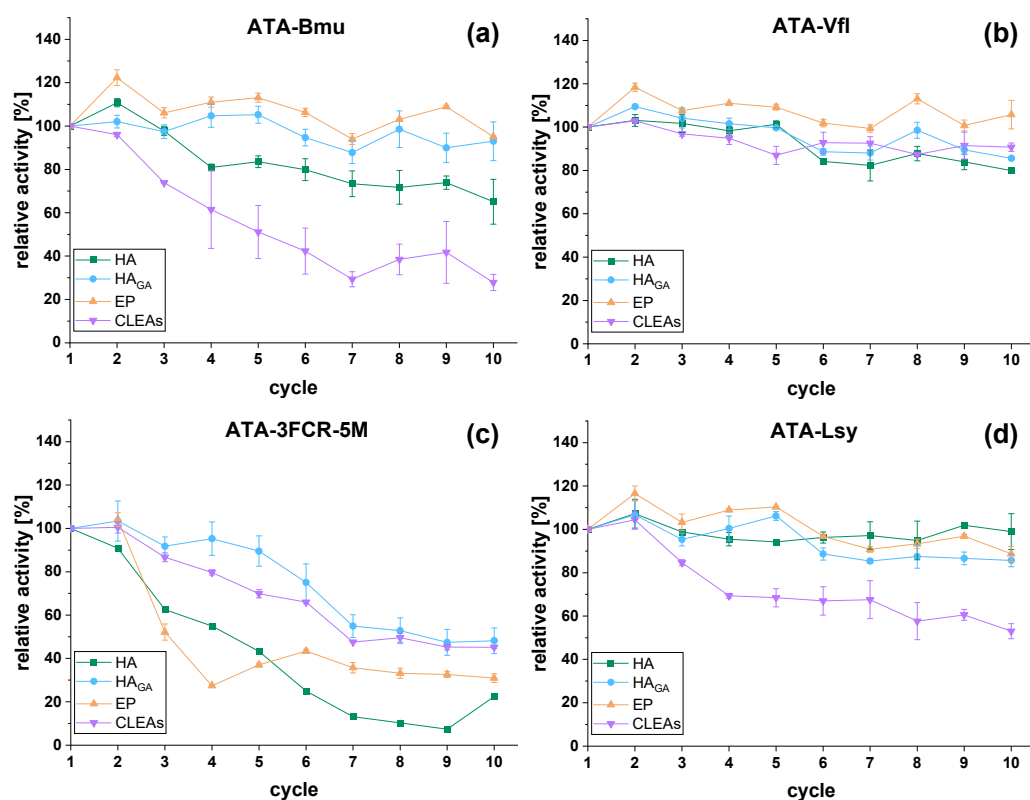


Figure 3. Recycling stability of different transaminase immobilizates. Various immobilizates of different transaminases (a) ATA-Bmu, (b) ATA-Vfl, (c) ATA-3FCR-5M, and (d) ATA-Lsy) were used in repeated kinetic resolutions of *rac*-1-PEA (2.5 mM) at 37 °C for 45 min each (50 mM Tris pH 8.0, 0.5% DMSO, 0.1 mM PLP, and 2.5 mM pyruvate). After each cycle, the supernatant was taken, the conversion was determined spectrophotometrically, and the immobilizates were washed (3 times with 50 mM Tris pH 8.0, 0.1 mM PLP), before fresh reaction solution was added. The initial activity of cycle 1 was set as 100%. All recycling studies were performed in duplicates, and the error bars of each average data point represent the minimum and maximum values.

For most enzymes, the immobilization via multipoint attachment may be favored for high recycling stabilities. Ultimately, we were able to present the immobilizates of all the transaminases of this study that can be used in at least 10 cycles, while maintaining full or high (ATA-3FCR-5M) activity. Immobilization via a single formylglycine residue per subunit was best for the hexameric ATA-Lsy. Notably, for ATA-Vfl, we achieved a higher recycling stability compared to other ATA-Vfl-immobilizates in the literature [46,53].

2.4. Upscaled Kinetic Resolution of *rac*-1-PEA Catalyzed by Immobilized Transaminases

Reactions are usually established on a small-scale to allow the rapid screening of different conditions. Upscaling raises issues such as mass transport, temperature control, or other limitations related to the enzymes used. Therefore, we aimed to demonstrate the scalability of the kinetic resolutions catalyzed by immobilized transaminases. The solid support yielding the highest specific activity of immobilizates for each transaminase was used (Table 1). The kinetic resolution was realized at 37 °C in a reaction volume of 110 mL, with 15 mM racemic 1-phenylethylamine, 15 mM pyruvate, and an appropriate amount of beads to obtain 15 units of immobilized transaminase (Table 1) to produce about 100 mg of enantiomerically pure 1-PEA. The reaction catalyzed by ATA-Lsy, immobilized on HA-beads, was performed in a SpinChem™ rotating bed reactor, which allows easy scaling by changing the reactor and/or vessel size, which is more comparable to industrial synthesis. The reactions catalyzed by ATA-Bmu, ATA-Vfl, and ATA-3FCR-5M, each immobilized on HA_{GA}-beads, were realized in 250 mL vessels. The SpinChem™ reactor could not be used because the HA_{GA}-beads leaked from the reactor (pore size of the mesh filter used in the reactor was about 100 μm), probably due to shrinkage during drying in the production of these beads. A complete conversion of the preferred enantiomer was observed in one day with (*R*)-1-PEA (ATA-Vfl, ATA-Bmu) or (*S*)-1-PEA (ATA-Lsy), as the remaining product in a high purity and a high yield as determined by chiral HPLC (Table 2, Figures S5 and S6). Small amounts of (*S*)-1-PEA remained unconverted with ATA-3FCR-5M-beads, which was the least stable immobilizate. Notably, the binding of 1-PEA and acetophenone to the beads was observed in different manners (Figure S7), potentially complicating the exact determination (especially of conversion and product yield).

Table 2. Upscaled kinetic resolution of *rac*-1-PEA catalyzed by immobilized transaminases. The best immobilizates of each transaminase (Table 1) were used in upscaled kinetic resolutions.

Transaminase	Type of Immobilization	Enantiomeric Excess [%ee] ^[a,c]	Obtained Enantiomer ^[a,c]	Product Yield [%] ^[b,c]
ATA-Bmu	HA _{GA}	98.8	(<i>R</i>)	72
ATA-Vfl	HA _{GA}	99.8	(<i>R</i>)	79
ATA-3FCR-5M	HA _{GA}	87.8	(<i>R</i>)	50
ATA-Lsy	HA	98.2	(<i>S</i>)	57

^[a] Data were obtained by chiral HPLC with extracted 1-PEA. ^[b] Net-weight of the extracted 1-PEA-enantiomer in relation to the expected amount of 100 mg. ^[c] Purity and structure of the extracted 1-PEA was verified by NMR analysis (Figure S6).

3. Materials and Methods

General information. All chemicals and solvents used were obtained mainly from commercial distributors of analytical grade: Merck, VWR, Carl Roth and Thermo Fisher Scientific. The amine (ReliZyme™, HA 403)- and epoxy (ReliZyme™, EP 403) beads were purchased in M-size from Resindion S.r.l.

Preparation of glutaraldehyde-functionalized amine (HA_{GA}) beads. HA-beads were washed (3 times 50 μL/mg bead with 100 mM phosphate buffer, pH 7.0) and then incubated with glutaraldehyde (5% solution in 50 mM phosphate buffer, pH 7.0) at 37 °C for 16 h. Afterwards, the beads were washed again (3 times phosphate buffer, 2 times water to remove salts) and dried under vacuum at 40 °C and 4.02 mbar for 2–3 h. The weight of the dried beads was related to the weight of the originally applied wet HA-beads to allow comparability.

Cloning of aldehyde-tag tagged transaminases. The aldehyde tag was inserted between the coding sequence of the transaminases and the His₆-tag (transaminase-AH), analogously to the cloning of ATA-Vfl-AH that performed previously [46]. The corresponding nucleic acid sequences, primers, and PCR programs are provided in the Supplementary Materials (Tables S3 and S4 and Section S6).

Expression and purification of $\Delta 72$ -hFGE. Expression of $\Delta 72$ -hFGE from insect cells was performed as described by Peng et al. [48]. After expression, the supernatant was dialyzed (2 times 12 h, 10-fold volume 25 mM Tris pH 8.0, and 100 mM NaCl), filtered (0.22 μm), and applied on a 1 mL HisTrapTM HP column (Ni^{2+} -NTA affinity chromatography, Cytiva), using the NGC system (BioRad) at 0.5 mL/min. Elution was performed using step gradients (5, 15, 18, 75, and 100% elution buffer (50 mM Tris pH 8.0, 150 mM NaCl, and 300 mM imidazole) in 50 mM Tris pH 8.0, 150 mM NaCl). The protein eluted at 225 mM imidazole was dialyzed directly (3 times 8 h, 200-fold volume of 25 mM Tris pH 8.0, and 100 mM NaCl), concentrated under vacuum (final concentration: 10 mg/mL), aliquoted, and stored at $-20\text{ }^{\circ}\text{C}$. Optimized purification yielded approximately 15–20 mg $\Delta 72$ -hFGE per liter medium. The chromatogram and SDS-gel are shown in Figure S8.

Expression and purification of transaminases. Heterologous protein expression in *E. coli* BL21(DE3) and purification by Ni^{2+} -NTA affinity chromatography on the NGC system (BioRad) was performed for all transaminases with and without aldehyde-tag in an analogous manner, as previously described for ATA-Vfl [89]. The nucleotide sequences of the tagged and untagged transaminases are provided in the Supplementary Materials (Section S7).

Aldehyde-tag conversion. To immobilize transaminase-AH mutants on HA-beads, the cysteine in the aldehyde-tag had to be converted to the unique formylglycine (FGly) by $\Delta 72$ -hFGE. For this purpose, 3 mM DTT followed by $\Delta 72$ -hFGE in a molar ratio of 1:30 ($\Delta 72$ -hFGE:transaminase) was added to the transaminase solutions (50 mM Tris pH 8.0, 0.1 mM PLP). Conversion was performed for 4 h at $37\text{ }^{\circ}\text{C}$ and proven by fluorescent-labeling (Figure S9). The preparations were used without further purification.

Fluorescent-labeling of C^{α} -formylglycine. A total of 20 μg protein was incubated with 0.1 mM Alexa FluorTM 488 Hydroxylamine at $22\text{ }^{\circ}\text{C}$ for 16 h under dark conditions in 20 μL of 250 mM citrate buffer at pH 3.6. Afterwards, the solutions were neutralized by adding 11 μL of 1 M NaOH, prepared for, and analyzed by SDS-PAGE, both under dark conditions. The in-gel fluorescence was detected (LAS-3000, Fujifilm, filter FL-Y515, excitation at 460 nm and emission at 515 nm) and was followed by Coomassie staining.

Immobilization of transaminases on solid supports. To establish optimal immobilization conditions, 5 mg beads and 20 μM transaminase solutions reacted at different pH values (5.0 (50 mM acetate buffer), 7.5 (50 mM sodium phosphate buffer), 9.0 (50 mM bicine buffer), and 10.5 (two buffers were analyzed, each 50 mM: CAPS and glycine/NaOH)) in 2 mL reaction vessels. To analyze the effect of different protein amounts (25, 50, 100, 150, and 200 μg per mg bead), suitable volumes were added. The immobilization was analyzed at different temperatures (4, 22, and $37\text{ }^{\circ}\text{C}$) for different durations (4, 8, 16, and 24 h). In the case of EP-beads, different additives were screened ($(\text{NH}_4)_2\text{SO}_4$ at different concentrations, 0.5 M sodium phosphate buffer pH 8.0, and 0.5 M NaCl). Except for the conditions varied in each case, standard conditions (50 mM bicine buffer, pH 9.0, 100 μg enzyme per mg bead, $37\text{ }^{\circ}\text{C}$, and 24 h) were maintained in each screening series. The immobilization buffers did not contain PLP to avoid competitive binding to the beads, which could result in the reduction of bound transaminases. Only in case of the HA-beads, the aldehyde-tagged transaminases with converted aldehyde-tag were used. After immobilization, the beads were washed (2 times 0.5 M NaCl, 2 times water) and blocked at $37\text{ }^{\circ}\text{C}$ for 1 h with 0.5 M glycine (EP-beads), 1 mM PLP (HA-beads), or 1 mM PLP with 0.5 M glycine (HA_{GA} -beads and all post-cross-linked beads), each in 50 mM bicine buffer pH 9.0. Afterwards, the beads were washed with water (3 times) and used for different approaches or stored in standard storage buffer (50 mM bicine pH 9.0, 0.1 mM PLP) under dark conditions until use. Determination of optimal immobilization conditions was performed in triplicates. Final immobilization was analogous to the above but it had appropriate amounts of beads and proteins under established immobilization conditions in 50 mL reaction vessels.

Immobilization of transaminases as CLEAs. To establish an optimal precipitant for each transaminase, 100 μL of a 10 μM transaminase solution was incubated with different precipitants (see Supplementary Materials) in 2 mL reaction vessels in a final volume of

500 μL (in phosphate buffer with a final concentration of 100 mM) at 4 $^{\circ}\text{C}$ for 1 h. Subsequently, the mixtures were centrifuged ($20,000\times g$), the supernatant discarded, and the protein pellet was resolubilized in bicine buffer (50 mM, pH 9.0, and 0.1 mM PLP). Protein concentration and transaminase activity were determined. To establish a sufficient cross-linker, the transaminases were precipitated with the four best precipitants (see Supplementary Materials) as mentioned above, after which, cross-linking with glutaraldehyde (GA) or divinylsulfone (DVS) at different concentrations (see Supplementary Materials) was allowed for additional 4 h at 4 $^{\circ}\text{C}$. After centrifugation ($20,000\times g$), the supernatant was discarded, the cross-linked protein pellet was suspended and washed in buffer (3 times 50 mM Tris pH 8.0, 0.1 mM PLP), and the activity of the formed CLEAs was determined. The establishment of precipitants and cross-linkers was performed at least in triplicates. For the final setups, CLEAs were prepared in appropriate volumes, as described above under the established conditions.

Activity assay of soluble transaminases. Racemic 1-phenylethylamine (*rac*-1-PEA) and pyruvate (2.5 mM each) were used to determine the activity of soluble transaminases by detecting the product, acetophenone, at 245 nm [71]. The reaction was performed in 96-well UV-microtiter plates (UV-Star[®], Greiner Bio-One) in the TECAN reader (Spark[™] 10M), with 1–10 μg protein per 150 μL reaction in the standard reaction buffer (50 mM Tris pH 8.0, 0.5% DMSO, 0.1 mM PLP) in duplicates. The concentration of acetophenone was calculated using the extinction coefficient of $12\text{ mM}^{-1}\text{ cm}^{-1}$ at 245 nm [71]. The activity of transaminases was determined using the average of 1 min differences within the initial reaction time (usually 5 min) to ensure the initial reaction velocity and linear slopes after start of the reaction by adding the substrates to the enzyme solution. The standard temperature was set at 37 $^{\circ}\text{C}$. To determine operational solvent activities, different solvents were added in different concentrations (further information can be obtained in the Supplementary Materials). A total of 1 unit was defined as the amount of soluble enzyme producing 1 μM acetophenone per minute at 37 $^{\circ}\text{C}$.

Discontinuous activity assay of immobilized transaminases. To determine the activity of immobilized transaminases, a discontinuous activity assay had to be performed. Therefore, 1.5 mL or 1.0 mL of reaction solution (50 mM Tris pH 8.0, 0.5% DMSO, 0.1 mM PLP, 2.5 mM *rac*-1-PEA, and 2.5 mM pyruvate) was used for 5 mg beads or for each CLEA-preparation, respectively. After a reaction time of 2 min at 37 $^{\circ}\text{C}$ (unless otherwise specified), 100 μL of the supernatant (always duplicates) was transferred to a 96-well UV-microtiter plate (UV-Star[®], Greiner Bio-One) and analyzed in the TECAN reader (Spark[™] 10 M) at 245 nm. The reaction time was set at 2 min to ensure determination within the initial reaction rates and linear slopes. All reactions were performed in sealed 2 mL vessels to avoid evaporation of acetophenone (Figure S7 and [89]). To determine operational solvent activities, different solvents were added in different concentrations (further information can be obtained in the Supplementary Materials). A total of 1 unit was defined as the amount of immobilized enzyme producing 1 μM acetophenone per minute at 37 $^{\circ}\text{C}$.

Determination of protein concentration. Total protein concentration was determined using the Bradford assay [90], with bovine serum albumin as the standard.

Analytical HPLC measurements. Analytical HPLC measurements were performed to determine the quantity of 1-PEA and acetophenone from reaction solutions, exactly as described previously [89].

Chiral HPLC measurements. The organic layers were subjected to chiral HPLC (Agilent 1100 series system with a Chiralcel OD column) using a short isocratic method (Mobile phase component A: *i*-PrOH, 0.2% *n*-butylamine; component B: *n*-hexane, 0.2% *n*-butylamine; 5% component A for 12 min, column oven: 40 $^{\circ}\text{C}$). Enantiomeric excess was determined by integration of the 254 nm UV-trace using the Mnova 14.3.0 software package.

Extraction of 1-PEA. The extraction was performed as described previously [89], except using DCM instead of *n*-Hexane to extract 1-PEA from the basified solutions. As some samples still contained trace amounts of DMSO, the yield was calculated after subtracting

the DMSO content as determined by NMR analysis in CDCl_3 . Enantiomeric excess of the isolated products was determined by chiral HPLC, as described previously.

NMR measurements. FT-NMR spectra were recorded using a Bruker Avance III 500 HD (^1H : 500 MHz, ^{13}C : 126 MHz) at 298 K, and the signals reported were relative to the solvent residual signal (DMSO: $\delta = 2.50$ ppm (^1H); $\delta = 39.52$ ppm (^{13}C). Analysis was performed using the Mnova 14.3.0 software package.

SDS-PAGE: The SDS-PAGE was performed exactly as described previously [89].

Immobilization parameters: Starting activity: The starting activity describes the total activity of the enzyme in the stock solution used for the immobilization procedure. Observed activity: The observed activity was the actual observed, directly measurable activity of the immobilized enzyme (immobilizate) under optimal conditions. Binding efficiency: Binding efficiency is described by the percentage ratio between the total amount of protein that is immobilized and the total amount of protein in the starting solution. The amount of immobilized protein is calculated by the difference between the amount in the starting solution minus the amount in the supernatant/wash solution. Activity recovery: The activity recovery describes the percentage ratio of observed activity to starting activity and thus, the relative amount of immobilized activity that was actually measured. In the above parameters, activity always indicates the total activity in the solution given in units. The activity was always determined under standard conditions at 37 °C, as mentioned in the methods.

The determination of the stability assays (i.e., thermo, storage, solvent, and recycling stability, Section S2), post-cross-linking, and drying of bead-immobilizates (Section S3) are comprehensively described in the Supplementary Materials.

4. Conclusions

In this study, four different transaminases from *Burkholderia multivorans* (ATA-Bmu), *Vibrio fluvialis* (ATA-Vfl), *Ruegeria* sp. TM1040 (variant: ATA-3FCR-5M), and *Luminiphilus sylltensis* NOR5-1B (ATA-Lsy), were successfully immobilized using four different strategies. It was found that the effects of immobilization were very heterogeneous: different immobilization strategies were optimal for different transaminases and applications. Multi-point immobilization via lysine residues onto glutaraldehyde-functionalized amine beads gave the highest specific activities for ATA-Bmu, ATA-Vfl, and ATA-3FCR-5M. Immobilization via a unique formylglycine residue per subunit to the amine beads resulted in the highest activity, an increased solvent tolerance, and increased recycling stability for ATA-Lsy. This may be due to the hexameric nature of this transaminase in contrast to dimeric ATA-Vfl and ATA-3FCR-5M and tetrameric ATA-Bmu. The storage stability of ATA-Bmu was greatly increased by all four immobilization methods. All immobilized transaminases could be efficiently recycled and used in upscaled kinetic resolution with maintained selectivity, high conversions, and high product yields.

Supplementary Materials: The following supporting information can be downloaded at: <https://www.mdpi.com/article/10.3390/catal13020300/s1>. Section S1: establishment of optimal immobilization conditions for each transaminase; Figure S1: establishment of optimal immobilization conditions Table S1: optimal immobilization conditions for each transaminase; immobilization parameters; Table S2: immobilization parameters; Section S2: methods and additional data on transaminase stability and activity; general setup of sample incubation [7,8,63,91,92]; Figure S2: stability and reactivity of ATA-Vfl, ATA-3FCR-5M, and ATA-Lsy under different conditions; Section S3: post-cross-linking and storage of dried beads; Figure S3: effect of post-cross-linking on specific activity of the immobilizates; Figure S4: effect of drying on specific activity of the immobilizates; Section S4: upscaled kinetic resolution catalyzed by the final immobilizates; Figure S5: chiral HPLC runs; Figure S6: exemplary NMR analysis of (S)-1-PEA.; Figure S7: behavior of acetophenone and 1-phenylethylamine in bead-containing solutions; Section S5: cloning of transaminases; Table S3: components and concentrations of the add-on and OE-PCR [46]; Table S4: PCR program for the add-on and OE-PCRs; Section S6: nucleic acid sequences; open reading frames of ATA-Bmu, ATA-3FCR-5M, and ATA-Lsy in respective plasmids w/o aldehyde-tag; open reading frames of ATA-Bmu, ATA-3FCR-5M, and

ATA-Lsy in pET24b-X-AH; Section S7: purification of $\Delta 72$ -hFGE; Figure S8: purification of $\Delta 72$ -hFGE; Section S8: fluorescent-labeling of FGly; Figure S9: fluorescent-labeling of formylglycine (exemplary for ATA-Vfl-AH); and Section S9: supporting references.

Author Contributions: Conceptualization, T.H.; methodology, T.H., N.M., M.T. and J.L.; validation, T.H., N.M. and M.T.; formal analysis, T.H., N.M., M.T. and J.L.; investigation, T.H., N.M., M.T. and J.L.; data curation, T.H.; writing—original draft preparation, T.H.; writing—review and editing, all authors.; visualization, T.H.; supervision, G.F.v.M., U.T.B. and M.H. All authors have read and agreed to the published version of the manuscript.

Funding: This research was funded by Bielefeld University.

Data Availability Statement: The data presented in this study are available in PUB (Publikationen an der Universität Bielefeld) at doi 10.4119/unibi/2968396.

Acknowledgments: We would like to thank Kerstin Glösenkamp (University of Bielefeld) for her technical support.

Conflicts of Interest: The authors declare no conflict of interest.

References

1. Savile, C.K.; Janey, J.M.; Mundorff, E.C.; Moore, J.C.; Tam, S.; Jarvis, W.R.; Colbeck, J.C.; Krebber, A.; Fleitz, F.J.; Brands, J.; et al. Biocatalytic asymmetric synthesis of chiral amines from ketones applied to sitagliptin manufacture. *Science* **2010**, *329*, 305–309. [[CrossRef](#)]
2. Fuchs, M.; Koszelewski, D.; Tauber, K.; Kroutil, W.; Faber, K. Chemoenzymatic asymmetric total synthesis of (S)-Rivastigmine using omega-transaminases. *Chem. Commun.* **2010**, *46*, 5500–5502. [[CrossRef](#)] [[PubMed](#)]
3. Busto, E.; Simon, R.C.; Grischek, B.; Gotor-Fernández, V.; Kroutil, W. Cutting short the asymmetric synthesis of the ramatroban precursor by employing ω -transaminases. *Adv. Synth. Catal.* **2014**, *356*, 1937–1942. [[CrossRef](#)]
4. Ghislieri, D.; Turner, N.J. Biocatalytic approaches to the synthesis of enantiomerically pure chiral amines. *Top. Catal.* **2014**, *57*, 284–300. [[CrossRef](#)]
5. Tufvesson, P.; Lima-Ramos, J.; Jensen, J.S.; Al-Haque, N.; Neto, W.; Woodley, J.M. Process considerations for the asymmetric synthesis of chiral amines using transaminases. *Biotechnol. Bioeng.* **2011**, *108*, 1479–1493. [[CrossRef](#)]
6. Singh, R.K.; Tiwari, M.K.; Singh, R.; Lee, J.-K. From protein engineering to immobilization: Promising strategies for the upgrade of industrial enzymes. *Int. J. Mol. Sci.* **2013**, *14*, 1232–1277. [[CrossRef](#)]
7. Börner, T.; Rämisch, S.; Reddem, E.R.; Bartsch, S.; Vogel, A.; Thunnissen, A.-M.W.H.; Adlercreutz, P.; Grey, C. Explaining operational instability of amine transaminases: Substrate-induced inactivation mechanism and influence of quaternary structure on enzyme–cofactor intermediate stability. *ACS Catal.* **2017**, *7*, 1259–1269. [[CrossRef](#)]
8. Chen, S.; Land, H.; Berglund, P.; Humble, M.S. Stabilization of an amine transaminase for biocatalysis. *J. Mol. Catal. B Enzym.* **2016**, *124*, 20–28. [[CrossRef](#)]
9. Guo, F.; Berglund, P. Transaminase biocatalysis: Optimization and application. *Green Chem.* **2017**, *19*, 333–360. [[CrossRef](#)]
10. Kelly, S.A.; Pohle, S.; Wharry, S.; Mix, S.; Allen, C.C.R.; Moody, T.S.; Gilmore, B.F. Application of ω -transaminases in the pharmaceutical industry. *Chem. Rev.* **2018**, *118*, 349–367. [[CrossRef](#)]
11. Truppo, M.D.; Strotman, H.; Hughes, G. Development of an immobilized transaminase capable of operating in organic solvent. *ChemCatChem* **2012**, *4*, 1071–1074. [[CrossRef](#)]
12. Rodrigues, R.C.; Ortiz, C.; Berenguer-Murcia, Á.; Torres, R.; Fernández-Lafuente, R. Modifying enzyme activity and selectivity by immobilization. *Chem. Soc. Rev.* **2013**, *42*, 6290–6307. [[CrossRef](#)]
13. Kaličanin, N.; Kovačević, G.; Spasojević, M.; Prodanović, O.; Jovanović-Šanta, S.; Škorić, D.; Opsenica, D.; Prodanović, R. Immobilization of ArRMut11 omega-transaminase for increased operational stability and reusability in the synthesis of 3 α -amino-5 α -androstan-17 β -ol. *Process. Biochem.* **2022**, *121*, 674–680. [[CrossRef](#)]
14. Liese, A.; Hilterhaus, L. Evaluation of immobilized enzymes for industrial applications. *Chem. Soc. Rev.* **2013**, *42*, 6236–6249. [[CrossRef](#)]
15. Bornscheuer, U.T. Immobilizing enzymes: How to create more suitable biocatalysts. *Angew. Chem. Int. Ed.* **2003**, *42*, 3336–3337. [[CrossRef](#)]
16. Neto, W.; Schürmann, M.; Panella, L.; Vogel, A.; Woodley, J.M. Immobilisation of ω -transaminase for industrial application: Screening and characterisation of commercial ready to use enzyme carriers. *J. Mol. Catal. B Enzym.* **2015**, *117*, 54–61. [[CrossRef](#)]
17. Velasco-Lozano, S.; Jackson, E.; Ripoll, M.; López-Gallego, F.; Betancor, L. Stabilization of ω -transaminase from *Pseudomonas fluorescens* by immobilization techniques. *Int. J. Biol. Macromol.* **2020**, *164*, 4318–4328. [[CrossRef](#)]
18. Deepankumar, K.; Nadarajan, S.P.; Mathew, S.; Lee, S.-G.; Yoo, T.H.; Hong, E.Y.; Kim, B.-G.; Yun, H. Engineering transaminase for stability enhancement and site-specific immobilization through multiple noncanonical amino acids incorporation. *ChemCatChem* **2015**, *7*, 417–421. [[CrossRef](#)]
19. Basso, A.; Serban, S. Industrial applications of immobilized enzymes—A review. *Mol. Catal.* **2019**, *479*, 110607. [[CrossRef](#)]

20. Fernandez-Lafuente, R. Stabilization of multimeric enzymes: Strategies to prevent subunit dissociation. *Enzym. Microb. Technol.* **2009**, *45*, 405–418. [[CrossRef](#)]
21. Carballares, D.; Morellon-Sterling, R.; Xu, X.; Hollmann, F.; Fernandez-Lafuente, R. Immobilization of the peroxygenase from *Agroclybe aegerita*. The effect of the immobilization pH on the features of an ionically exchanged dimeric peroxygenase. *Catalysts* **2021**, *11*, 560. [[CrossRef](#)]
22. Deshmukh, S.S.; Dutta Choudhury, M.; Shankar, V. Preparation and properties of glucose isomerase immobilized on Indion 48-R. *Appl. Biochem. Biotechnol.* **1993**, *42*, 95–104. [[CrossRef](#)]
23. Kappauf, K.; Majstorovic, N.; Agarwal, S.; Rother, D.; Claaßen, C. Modulation of transaminase activity by encapsulation in temperature-sensitive poly(N-acryloyl glycinamide) hydrogels. *ChemBioChem* **2021**, *22*, 3452–3461. [[CrossRef](#)]
24. Talekar, S.; Joshi, A.; Joshi, G.; Kamat, P.; Haripurkar, R.; Kambale, S. Parameters in preparation and characterization of cross linked enzyme aggregates (CLEAs). *RSC Adv.* **2013**, *3*, 12485–12511. [[CrossRef](#)]
25. Roy, I.; Mukherjee, J.; Gupta, M.N. Cross-linked enzyme aggregates for applications in aqueous and nonaqueous media. *Methods Mol. Biol.* **2017**, *1504*, 109–123. [[CrossRef](#)]
26. Rojas, M.; Amaral-Fonseca, M.; Zanin, G.; Fernandez-Lafuente, R.; Giordano, R.; Tardioli, P. Preparation of crosslinked enzyme aggregates of a thermostable cyclodextrin glucosyltransferase from *Thermoanaerobacter* sp. critical effect of the crosslinking agent. *Catalysts* **2019**, *9*, 120. [[CrossRef](#)]
27. Yamaguchi, H.; Kiyota, Y.; Miyazaki, M. Techniques for preparation of cross-linked enzyme aggregates and their applications in bioconversions. *Catalysts* **2018**, *8*, 174. [[CrossRef](#)]
28. Kahar, U.M.; Sani, M.H.; Chan, K.-G.; Goh, K.M. Immobilization of α -amylase from *Anoxybacillus* sp. SK3-4 on ReliZyme and imbead supports. *Molecules* **2016**, *21*, 1196. [[CrossRef](#)] [[PubMed](#)]
29. López-Gallego, F.; Guisan, J.M.; Betancor, L. Immobilization of enzymes on supports activated with glutaraldehyde: A very simple immobilization protocol. *Methods Mol. Biol.* **2020**, *2100*, 119–127. [[CrossRef](#)] [[PubMed](#)]
30. Betancor, L.; López-Gallego, F.; Hidalgo, A.; Alonso-Morales, N.; Dellamora-Ortiz, G.M.; Fernández-Lafuente, R.; Guisán, J.M. Different mechanisms of protein immobilization on glutaraldehyde activated supports: Effect of support activation and immobilization conditions. *Enzym. Microb. Technol.* **2006**, *39*, 877–882. [[CrossRef](#)]
31. Bezbradica, D.I.; Mateo, C.; Guisan, J.M. Novel support for enzyme immobilization prepared by chemical activation with cysteine and glutaraldehyde. *J. Mol. Catal. B Enzym.* **2014**, *102*, 218–224. [[CrossRef](#)]
32. De Souza, S.P.; Junior, I.I.; Silva, G.M.A.; Miranda, L.S.M.; Santiago, M.F.; Leung-Yuk Lam, F.; Dawood, A.; Bornscheuer, U.T.; de Souza, R.O.M.A. Cellulose as an efficient matrix for lipase and transaminase immobilization. *RSC Adv.* **2016**, *6*, 6665–6671. [[CrossRef](#)]
33. Mallin, H.; Höhne, M.; Bornscheuer, U.T. Immobilization of (R)- and (S)-amine transaminases on chitosan support and their application for amine synthesis using isopropylamine as donor. *J. Biotechnol.* **2014**, *191*, 32–37. [[CrossRef](#)] [[PubMed](#)]
34. Jia, D.-X.; Xu, H.-P.; Sun, C.-Y.; Peng, C.; Li, J.-L.; Jin, L.-Q.; Cheng, F.; Liu, Z.-Q.; Xue, Y.-P.; Zheng, Y.-G. Covalent immobilization of recombinant *Citrobacter koseri* transaminase onto epoxy resins for consecutive asymmetric synthesis of l-phosphinothricin. *Bioprocess. Biosyst. Eng.* **2020**, *43*, 1599–1607. [[CrossRef](#)]
35. Abaházi, E.; Sátorhelyi, P.; Erdélyi, B.; Vértessy, B.G.; Land, H.; Paizs, C.; Berglund, P.; Poppe, L. Covalently immobilized Trp60Cys mutant of ω -transaminase from *Chromobacterium violaceum* for kinetic resolution of racemic amines in batch and continuous-flow modes. *Biochem. Eng. J.* **2018**, *132*, 270–278. [[CrossRef](#)]
36. Bilgin, R.; Yalcin, M.S.; Yildirim, D. Optimization of covalent immobilization of *Trichoderma reesei* cellulase onto modified ReliZyme HA403 and Sepabeads EC-EP supports for cellulose hydrolysis, in buffer and ionic liquids/buffer media. *Artif. Cells Nanomed. Biotechnol.* **2016**, *44*, 1276–1284. [[CrossRef](#)] [[PubMed](#)]
37. Bayraktar, H.; Serilmez, M.; Karkas, T.; Celep, E.B.; Onal, S. Immobilization and stabilization of α -galactosidase on Sepabeads EC-EA and EC-HA. *Int. J. Biol. Macromol.* **2011**, *49*, 855–860. [[CrossRef](#)] [[PubMed](#)]
38. Yepes, C.; Estévez, J.; Arroyo, M.; Ladero, M. Immobilization of an industrial β -glucosidase from *Aspergillus fumigatus* and its use for cellobiose hydrolysis. *Processes* **2022**, *10*, 1225. [[CrossRef](#)]
39. Nagy, F.; Gyujto, I.; Tasnádi, G.; Barna, B.; Balogh-Weiser, D.; Faber, K.; Poppe, L.; Hall, M. Design and application of a bi-functional redox biocatalyst through covalent co-immobilization of ene-reductase and glucose dehydrogenase. *J. Biotechnol.* **2020**, *323*, 246–253. [[CrossRef](#)]
40. Wang, X.; Xie, Y.; Wang, Z.; Zhang, K.; Wang, H.; Wei, D. Efficient synthesis of (S)-1-boc-3-aminopiperidine in a continuous flow system using ω -transaminase-immobilized amino-ethylenediamine-modified epoxide supports. *Org. Process. Res. Dev.* **2022**, *26*, 1351–1359. [[CrossRef](#)]
41. Li, M.; Cheng, F.; Li, H.; Jin, W.; Chen, C.; He, W.; Cheng, G.; Wang, Q. Site-specific and covalent immobilization of His-tagged proteins via surface vinyl sulfone-imidazole coupling. *Langmuir* **2019**, *35*, 16466–16475. [[CrossRef](#)] [[PubMed](#)]
42. Ley, C.; Holtmann, D.; Mangold, K.-M.; Schrader, J. Immobilization of histidine-tagged proteins on electrodes. *Colloids Surf. B Biointerfaces* **2011**, *88*, 539–551. [[CrossRef](#)]
43. Zhong, M.; Fang, J.; Wei, Y. Site specific and reversible protein immobilization facilitated by a DNA binding fusion tag. *Bioconjugate Chem.* **2010**, *21*, 1177–1182. [[CrossRef](#)] [[PubMed](#)]

44. Wang, J.-H.; Tang, M.-Z.; Yu, X.-T.; Xu, C.-M.; Yang, H.-M.; Tang, J.-B. Site-specific, covalent immobilization of an engineered enterokinase onto magnetic nanoparticles through transglutaminase-catalyzed bioconjugation. *Colloids Surf. B Biointerfaces* **2019**, *177*, 506–511. [[CrossRef](#)] [[PubMed](#)]
45. Camarero, J.A. Recent developments in the site-specific immobilization of proteins onto solid supports. *Biopolymers* **2008**, *90*, 450–458. [[CrossRef](#)] [[PubMed](#)]
46. Janson, N.; Heinks, T.; Beuel, T.; Alam, S.; Höhne, M.; Bornscheuer, U.T.; von Mollard, G.F.; Sewald, N. Efficient site-selective immobilization of aldehyde-tagged peptides and proteins by knoevenagel ligation. *ChemCatChem* **2022**, *14*, e202101485. [[CrossRef](#)]
47. Raliski, B.K.; Howard, C.A.; Young, D.D. Site-specific protein immobilization using unnatural amino acids. *Bioconjugate Chem.* **2014**, *25*, 1916–1920. [[CrossRef](#)]
48. Peng, J.; Alam, S.; Radhakrishnan, K.; Mariappan, M.; Rudolph, M.G.; May, C.; Dierks, T.; von Figura, K.; Schmidt, B. Eukaryotic formylglycine-generating enzyme catalyses a monooxygenase type of reaction. *FEBS J.* **2015**, *282*, 3262–3274. [[CrossRef](#)] [[PubMed](#)]
49. Dierks, T.; Lecca, M.R.; Schlotterhose, P.; Schmidt, B.; von Figura, K. Sequence determinants directing conversion of cysteine to formylglycine in eukaryotic sulfatases. *EMBO J.* **1999**, *18*, 2084–2091. [[CrossRef](#)]
50. Peng, Q.; Zang, B.; Zhao, W.; Li, D.; Ren, J.; Ji, F.; Jia, L. Efficient continuous-flow aldehyde tag conversion using immobilized formylglycine generating enzyme. *Catal. Sci. Technol.* **2020**, *10*, 484–492. [[CrossRef](#)]
51. Ju, W.; Zhen, X.; Zheng, L. Soluble expression and biomimetic immobilization of a ω -transaminase from *Bacillus subtilis*: Development of an efficient and recyclable biocatalyst. *Biochem. Eng. J.* **2020**, *160*, 107635. [[CrossRef](#)]
52. Böhmer, W.; Knaus, T.; Volkov, A.; Slot, T.K.; Shiju, N.R.; Cassimjee, K.E.; Mutti, F.G. Highly efficient production of chiral amines in batch and continuous flow by immobilized ω -transaminases on controlled porosity glass metal-ion affinity carrier. *J. Biotechnol.* **2019**, *291*, 52–60. [[CrossRef](#)] [[PubMed](#)]
53. Yi, S.-S.; Lee, C.; Kim, J.; Kyung, D.; Kim, B.-G.; Lee, Y.-S. Covalent immobilization of ω -transaminase from *Vibrio fluvialis* JS17 on chitosan beads. *Process. Biochem.* **2007**, *42*, 895–898. [[CrossRef](#)]
54. Molnár, Z.; Farkas, E.; Lakó, Á.; Erdélyi, B.; Kroutil, W.; Vértessy, B.G.; Paizs, C.; Poppe, L. Immobilized whole-cell transaminase biocatalysts for continuous-flow kinetic resolution of amines. *Catalysts* **2019**, *9*, 438. [[CrossRef](#)]
55. Cárdenas-Fernández, M.; Neto, W.; López, C.; Álvaro, G.; Tufvesson, P.; Woodley, J.M. Immobilization of *Escherichia coli* containing ω -transaminase activity in LentiKats[®]. *Biotechnol. Prog.* **2012**, *28*, 693–698. [[CrossRef](#)]
56. Mallin, H.; Menyes, U.; Vorhaben, T.; Höhne, M.; Bornscheuer, U.T. Immobilization of two (R)-amine transaminases on an optimized chitosan support for the enzymatic synthesis of optically pure amines. *ChemCatChem* **2013**, *5*, 588–593. [[CrossRef](#)]
57. Martin, A.R.; Shonnard, D.; Pannuri, S.; Kamat, S. Characterization of free and immobilized (S)-aminotransferase for acetophenone production. *Appl. Microbiol. Biotechnol.* **2007**, *76*, 843–851. [[CrossRef](#)]
58. Ni, K.; Zhou, X.; Zhao, L.; Wang, H.; Ren, Y.; Wei, D. Magnetic catechol-chitosan with bioinspired adhesive surface: Preparation and immobilization of ω -transaminase. *PLoS ONE* **2012**, *7*, e41101. [[CrossRef](#)]
59. Semproli, R.; Vaccaro, G.; Ferrandi, E.E.; Vanoni, M.; Bavaro, T.; Marrubini, G.; Annunziata, F.; Conti, P.; Speranza, G.; Monti, D.; et al. Use of immobilized amine transaminase from *Vibrio fluvialis* under flow conditions for the synthesis of (S)-1-(5-fluoropyrimidin-2-yl)-ethanamine. *ChemCatChem* **2020**, *12*, 1359–1367. [[CrossRef](#)]
60. Genz, M.; Vickers, C.; van den Bergh, T.; Joosten, H.-J.; Dörr, M.; Höhne, M.; Bornscheuer, U.T. Alteration of the donor/acceptor spectrum of the (S)-amine transaminase from *Vibrio fluvialis*. *Int. J. Mol. Sci.* **2015**, *16*, 26953–26963. [[CrossRef](#)] [[PubMed](#)]
61. Shin, Y.-C.; Yun, H.; Park, H.H. Structural dynamics of the transaminase active site revealed by the crystal structure of a co-factor free omega-transaminase from *Vibrio fluvialis* JS17. *Sci. Rep.* **2018**, *8*, 11454. [[CrossRef](#)] [[PubMed](#)]
62. Genz, M.; Melse, O.; Schmidt, S.; Vickers, C.; Dörr, M.; van den Bergh, T.; Joosten, H.-J.; Bornscheuer, U.T. Engineering the amine transaminase from *Vibrio fluvialis* towards branched-chain substrates. *ChemCatChem* **2016**, *8*, 3199–3202. [[CrossRef](#)]
63. Chen, S.; Campillo-Brocal, J.C.; Berglund, P.; Humble, M.S. Characterization of the stability of *Vibrio fluvialis* JS17 amine transaminase. *J. Biotechnol.* **2018**, *282*, 10–17. [[CrossRef](#)] [[PubMed](#)]
64. Shin, J.-S.; Yun, H.; Jang, J.-W.; Park, I.; Kim, B.-G. Purification, characterization, and molecular cloning of a novel amine:pyruvate transaminase from *Vibrio fluvialis* JS17. *Appl. Microbiol. Biotechnol.* **2003**, *61*, 463–471. [[CrossRef](#)] [[PubMed](#)]
65. Kollipara, M.; Matzel, P.; Sowa, M.; Brott, S.; Bornscheuer, U.; Höhne, M. Characterization of proteins from the 3N5M family reveals an operationally stable amine transaminase. *Appl. Microbiol. Biotechnol.* **2022**, *106*, 5563–5574. [[CrossRef](#)]
66. Steffen-Munsberg, F.; Vickers, C.; Thontowi, A.; Schätzle, S.; Meinhardt, T.; Svedendahl Humble, M.; Land, H.; Berglund, P.; Bornscheuer, U.T.; Höhne, M. Revealing the structural basis of promiscuous amine transaminase activity. *ChemCatChem* **2013**, *5*, 154–157. [[CrossRef](#)]
67. Steffen-Munsberg, F.; Vickers, C.; Thontowi, A.; Schätzle, S.; Tumlirsch, T.; Svedendahl Humble, M.; Land, H.; Berglund, P.; Bornscheuer, U.T.; Höhne, M. Connecting unexplored protein crystal structures to enzymatic function. *ChemCatChem* **2013**, *5*, 150–153. [[CrossRef](#)]
68. Pavlidis, I.V.; Weiß, M.S.; Genz, M.; Spurr, P.; Hanlon, S.P.; Wirz, B.; Iding, H.; Bornscheuer, U.T. Identification of (S)-selective transaminases for the asymmetric synthesis of bulky chiral amines. *Nat. Chem.* **2016**, *8*, 1076–1082. [[CrossRef](#)]
69. Höhne, M.; Schätzle, S.; Jochens, H.; Robins, K.; Bornscheuer, U.T. Rational assignment of key motifs for function guides in silico enzyme identification. *Nat. Chem. Biol.* **2010**, *6*, 807–813. [[CrossRef](#)]

70. Konia, E.; Chatzicharalampous, K.; Drakonaki, A.; Muenke, C.; Ermler, U.; Tsiotis, G.; Pavlidis, I.V. Rational engineering of Luminiphilus sylvensis (R)-selective amine transaminase for the acceptance of bulky substrates. *Chem. Commun.* **2021**, *57*, 12948–12951. [[CrossRef](#)]
71. Schätzle, S.; Höhne, M.; Redestad, E.; Robins, K.; Bornscheuer, U.T. Rapid and sensitive kinetic assay for characterization of omega-transaminases. *Anal. Chem.* **2009**, *81*, 8244–8248. [[CrossRef](#)] [[PubMed](#)]
72. Yang, A.S.; Honig, B. On the pH dependence of protein stability. *J. Mol. Biol.* **1993**, *231*, 459–474. [[CrossRef](#)] [[PubMed](#)]
73. Mazzini, A.; Polverini, E.; Parisi, M.; Sorbi, R.T.; Favilla, R. Dissociation and unfolding of bovine odorant binding protein at acidic pH. *J. Struct. Biol.* **2007**, *159*, 82–91. [[CrossRef](#)] [[PubMed](#)]
74. Guranda, D.T.; Volovik, T.S.; Svedas, V.K. pH stability of penicillin acylase from Escherichia coli. *Biochemistry Mosc.* **2004**, *69*, 1386–1390. [[CrossRef](#)] [[PubMed](#)]
75. López-Gallego, F.; Fernandez-Lorente, G.; Rocha-Martin, J.; Bolivar, J.M.; Mateo, C.; Guisan, J.M. Stabilization of enzymes by multipoint covalent immobilization on supports activated with glyoxyl groups. *Methods Mol. Biol.* **2013**, *1051*, 59–71. [[CrossRef](#)] [[PubMed](#)]
76. Guisan, J.M.; Fernandez-Lorente, G.; Rocha-Martin, J.; Moreno-Gamero, D. Enzyme immobilization strategies for the design of robust and efficient biocatalysts. *Curr. Opin. Green Sustain. Chem.* **2022**, *35*, 100593. [[CrossRef](#)]
77. Wang, B.; Zhou, J.; Zhang, X.-Y.; Yang, Y.-S.; Liu, C.-H.; Zhu, H.-L.; Jiao, Q.-C. Covalently immobilize crude d-amino acid transaminase onto UiO-66-NH₂ surface for d-Ala biosynthesis. *Int. J. Biol. Macromol.* **2021**, *175*, 451–458. [[CrossRef](#)]
78. Zhang, X.-J.; Fan, H.-H.; Liu, N.; Wang, X.-X.; Cheng, F.; Liu, Z.-Q.; Zheng, Y.-G. A novel self-sufficient biocatalyst based on transaminase and pyridoxal 5'-phosphate covalent co-immobilization and its application in continuous biosynthesis of sitagliptin. *Enzym. Microb. Technol.* **2019**, *130*, 109362. [[CrossRef](#)]
79. Shin, J.-S.; Kim, B.-G.; Shin, D.-H. Kinetic resolution of chiral amines using packed-bed reactor. *Enzyme Microb. Technol.* **2001**, *29*, 232–239. [[CrossRef](#)]
80. Koszelewski, D.; Müller, N.; Schrittwieser, J.H.; Faber, K.; Kroutil, W. Immobilization of ω -transaminases by encapsulation in a sol-gel/celite matrix. *J. Mol. Catal. B Enzym.* **2010**, *63*, 39–44. [[CrossRef](#)]
81. Wang, C.; Tang, K.; Dai, Y.; Jia, H.; Li, Y.; Gao, Z.; Wu, B. Identification, characterization, and site-specific mutagenesis of a thermostable ω -transaminase from *Chloroflexi bacterium*. *ACS Omega* **2021**, *6*, 17058–17070. [[CrossRef](#)] [[PubMed](#)]
82. Ferrandi, E.E.; Previdi, A.; Bassanini, I.; Riva, S.; Peng, X.; Monti, D. Novel thermostable amine transferases from hot spring metagenomes. *Appl. Microbiol. Biotechnol.* **2017**, *101*, 4963–4979. [[CrossRef](#)] [[PubMed](#)]
83. Tang, K.; Yi, Y.; Gao, Z.; Jia, H.; Li, Y.; Cao, F.; Zhou, H.; Jiang, M.; Wei, P. Identification, heterologous expression and characterization of a transaminase from *Rhizobium* sp. *Catal. Lett.* **2020**, *150*, 2415–2426. [[CrossRef](#)]
84. Tentori, F.; Brenna, E.; Crotti, M.; Pedrocchi-Fantoni, G.; Ghezzi, M.C.; Tessaro, D. Continuous-flow biocatalytic process for the synthesis of the best stereoisomers of the commercial fragrances leather cyclohexanol (4-isopropylcyclohexanol) and woody acetate (4-(tert-butyl)cyclohexyl acetate). *Catalysts* **2020**, *10*, 102. [[CrossRef](#)]
85. Weltz, J.S.; Kienle, D.F.; Schwartz, D.K.; Kaar, J.L. Reduced enzyme dynamics upon multipoint covalent immobilization leads to dtability-activity trade-off. *J. Am. Chem. Soc.* **2020**, *142*, 3463–3471. [[CrossRef](#)]
86. Rodrigues, R.C.; Berenguer-Murcia, Á.; Carballares, D.; Morellon-Sterling, R.; Fernandez-Lafuente, R. Stabilization of enzymes via immobilization: Multipoint covalent attachment and other stabilization strategies. *Biotechnol. Adv.* **2021**, *52*, 107821. [[CrossRef](#)]
87. Ruggieri, F.; Campillo-Brocal, J.C.; Chen, S.; Humble, M.S.; Walse, B.; Logan, D.T.; Berglund, P. Insight into the dimer dissociation process of the Chromobacterium violaceum (S)-selective amine transaminase. *Sci. Rep.* **2019**, *9*, 16946. [[CrossRef](#)]
88. Börner, T.; Rämisch, S.; Bartsch, S.; Vogel, A.; Adlercreutz, P.; Grey, C. Three in one: Temperature, solvent and catalytic stability by engineering the cofactor-binding element of amine transaminase. *ChemBioChem* **2017**, *18*, 1482–1486. [[CrossRef](#)]
89. Heinks, T.; Paulus, J.; Koopmeiners, S.; Beuel, T.; Sewald, N.; Höhne, M.; Bornscheuer, U.T.; Fischer von Mollard, G. Recombinant l-amino acid oxidase with broad substrate spectrum for co-substrate recycling in (S)-selective transaminase-catalyzed kinetic resolutions. *ChemBioChem* **2022**, *23*, e202200329. [[CrossRef](#)]
90. Bradford, M.M. A rapid and sensitive method for the quantitation of microgram quantities of protein utilizing the principle of protein-dye binding. *Anal. Biochem.* **1976**, *72*, 248–254. [[CrossRef](#)]
91. Merz, L.M.; van Langen, L.M.; Berglund, P. The role of buffer, pyridoxal 5'-phosphate and light on the stability of the *Silicibacter pomeroyi* transaminase. *ChemCatChem* **2022**, e202201174. [[CrossRef](#)]
92. Seo, J.-H.; Kyung, D.; Joo, K.; Lee, J.; Kim, B.-G. Necessary and sufficient conditions for the asymmetric synthesis of chiral amines using ω -aminotransferases. *Biotechnol. Bioeng.* **2011**, *108*, 253–263. [[CrossRef](#)] [[PubMed](#)]

Disclaimer/Publisher's Note: The statements, opinions and data contained in all publications are solely those of the individual author(s) and contributor(s) and not of MDPI and/or the editor(s). MDPI and/or the editor(s) disclaim responsibility for any injury to people or property resulting from any ideas, methods, instructions or products referred to in the content.